Article

Comparative Studies of the Corrosion Inhibition Efficacy of a Dicationic Monomer and Its Polymer against API X60 Steel Corrosion in Simulated Acidizing Fluid under Static and Hydrodynamic Conditions

Nurudeen A. Odewunmi, Moses M. Solomon, Saviour A. Umoren,* and Shaikh A. Ali*

Cite This: ACS Omega 2020, 5, 27057−27071

Read Online

ACCESS | Metrics & More | Article Recommendations | Supporting Information

ABSTRACT: N^1,N^1-diallyl-N^6,N^6,N^6-tripropylhexane-1,6-diaminium chloride (NDTHDC) and its polymer poly(N^1,N^1-diallyl-N^6,N^6,N^6-tripropylhexane-1,6-diaminium chloride) (poly-NDTHDC) were synthesized and tested against API X60 carbon steel corrosion in 15 wt % HCl solution. Weight loss, electrochemical, and surface analysis techniques were used. Results show that poly-NDTHDC is better than NDTHDC. Moreover, 1000 mg/L NDTHDC protected the studied surface by 79.1% at 25 °C, while 100 mg/L poly-NDTHDC afforded 86.1% protection. Inhibition efficiency increases with temperature (up to 60 °C) but depreciates thereafter. NDTHDC and poly-NDTHDC perform better under the hydrodynamic condition than the static condition. TGA and FTIR results reveal that poly-NDTHDC is chemically and thermally stable.
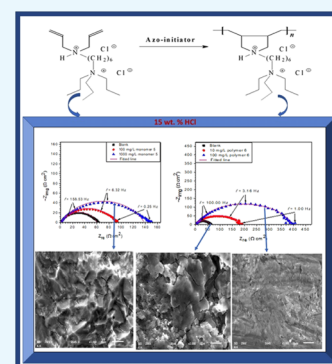
1. INTRODUCTION

Since the dawn of the oil and gas industry, operators have devised several techniques to maximize well production. Matrix acidizing is one of such techniques and is meant to increase fluid production by enhancing the drainage efficiency of the reservoir rock around the wellbore.[1] It entails the pumping of concentrated acid solution into an oil well to dissolve and remove formation damage, resulting from drilling and completion operations, and to create new production pathways in production formations.[1] Nevertheless, corrosion of well tubings, which are mostly fabricated from API-grade low carbon steels, is one of the problems associated with well acidizing.[2,3] A suitable, reliable, and cost-effective corrosion mitigation approach is the corrosion inhibitor technology,[3−6] which involves the addition of corrosion inhibitors to the acid solution. The inhibitors must offer effective protection to the tubings for at least 2 h while the acid is being pumped into the producing formation[4] and up to 24 h in a situation when the acid is used as a perforating fluid.[4]

The commercial inhibitors used in stimulation acids are complex proprietary formulations that frequently contain quaternary heterocyclic ammonium salts and halogenated compounds that work in synergy with propargyl alcohol, which is known to be extremely poisonous.[2,7] Propargyl alcohol, an alcohol containing an alkyne functional group, has a lethal dose (LD$_{50}$) value of 20 mg/kg, an acute oral toxicity classification of category 3, and a chronic aquatic toxicity of category 2, according to the GHS classification.[8,9] Because

government policies have continued to promote green alternatives to toxic petrochemicals, research efforts toward the development of green corrosion inhibitors have intensified in recent times. It was reported[2,10] that eco-friendly indolizine derivatives synthesized from quinoline, pyridine, and halide compounds through a 1,3-dipolar cycloaddition reaction effectively inhibited the corrosion of N80 steel in 15 wt % HCl and 20 wt % HCl solutions. With 0.1 wt % of the indolizine derivatives, inhibition efficiency as high as 99% was reported at 90 °C. Pyran derivatives had equally been documented as effective and nontoxic acidizing corrosion inhibitors.[11]

Bis-ammonium salts are less expensive and environmentally friendly surfactants;[5,6] many have been synthesized and tested as corrosion inhibitors.[5,6] Depending on the application conditions, they are effective in retarding metal corrosions.[5,6] Zhang et al.[6] however reported that the corrosion inhibition performance of bis-ammonium salts depreciates at high temperatures, and as such, a large dosage is required. Typically, inhibitor concentration in the range of 1000−5000 ppm is used in the acidization process.[12] It had been shown that, due
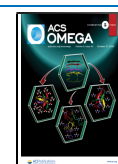
to the presence of multiple adsorption sites, polymers perform better as corrosion inhibitors than their corresponding monomers.[13] In this work, a bis-ammonium salt was synthesized and evaluated as a corrosion inhibitor for API X60 carbon steel in a 15 wt % HCl solution. The effect of polymerization, temperature (25, 60, and 90 °C), and flow (500, 1000, and 1500 rpm) on the corrosion inhibition performance of the synthesized bis-ammonium salt was also studied. The thermal and chemical stabilities of the polymer in 15 wt % HCl solution heated at 90 °C for 12 h was equally studied using thermogravimetric analysis and Fourier transform infrared spectroscopy (FTIR). Studies on these important secondary properties of corrosion inhibitors are lacking in the corrosion literature. Different techniques including weight loss, electrochemical (electrochemical impedance spectroscopy, linear polarization resistance, and potentiodynamic polarization), and surface characterization (scanning electron microscope (SEM), atomic force microscopy (AFM), FTIR, contact angle, and UV−vis) were used in the investigation.

2. RESULTS AND DISCUSSION

2.1. Synthesis and Confirmation of NDTHDC and Poly-NDTHDC.
Alkylation of diallylamine **4** with the bromide salt **3**[13,14] followed by Cl⁻ ions' exchange with Br⁻ ions afforded the dicationic NDTHDC in excellent yield (Scheme 1). NDTHDC upon cyclopolymerization using Butler's

Scheme 1. Syntheses of a Dicationic NDTHDC and its Poly-NDTHDC
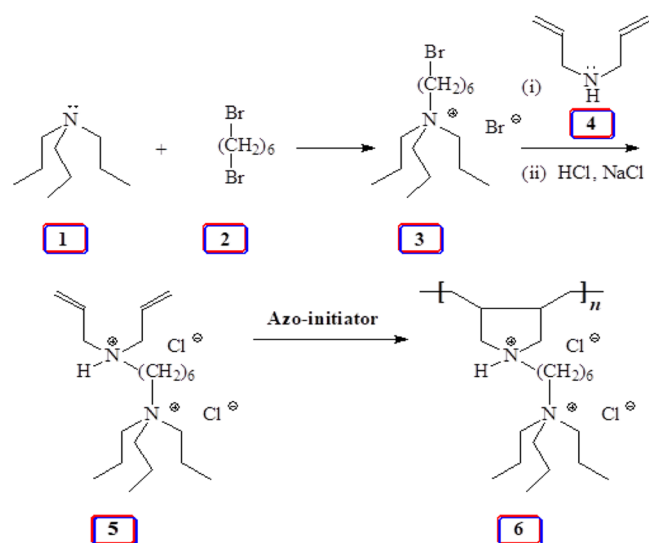
cyclopolymerization protocol[13,15−18] in the presence of the initiator, 2,2′-azobis(2-methylpropionamidine) dihydrochloride, gave cyclopoly-NDTHDC as a creamy solid (Scheme 1). The ¹H and ¹³C NMR spectra of NDTHDC and its corresponding poly-NDTHDC are shown in Figures S1 and S2 in the Supporting Information. The disappearance of the alkene protons and alkene carbons seen in the ¹H (Figure S1a) and ¹³C (Figure S2a) NMR spectra of NDTHDC in Figures S1b and S2b, respectively, confirms the formation of poly-NDTHDC.

2.2. Weight-Loss Studies.
The variation of corrosion rate and inhibition efficiency with different concentrations of (a) NDTHDC and (b) poly-NDTHDC in 15 wt % HCl solution

at 25 °C is shown in Figure 1. It is clear from the figure that the corrosion rate was the highest in the uninhibited acid
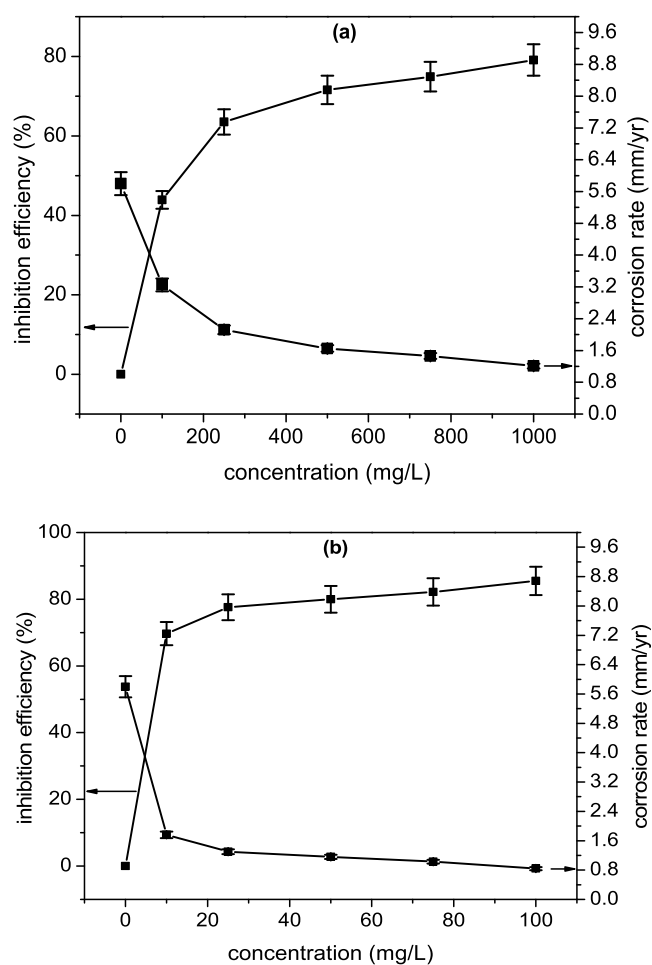

Figure 1. Variation of the corrosion rate and inhibition efficiency with concentration of (a) NDTHDC and (b) poly-NDTHDC in 15 wt % HCl solution at 25 °C.

solution but significantly reduced upon the addition of the inhibitor. In the absence of an inhibitor, the steel specimen corroded at a rate of 5.80 mm/year but was reduced to 3.25 and 1.76 mm/year upon addition of 100 mg/L NDTHDC and 10 mg/L poly-NDTHDC, respectively. This translated to inhibition efficiencies of 43.9 and 69.7% by 100 mg/L NDTHDC and 10 mg/L poly-NDTHDC, respectively. This observation could be due to the blockage of the corrosion reaction sites by adsorbed inhibitor molecules, which eventually delayed the corrosion process.[13,19] However, it is observed that the influence of NDTHDC and poly-NDTHDC is a function of concentration. That is, the corrosion rate decreases while the inhibition efficiency increases with an increase in the concentration of NDTHDC and poly-NDTHDC. This could be due to greater surface coverage.[19]

A close inspection of Figure 1b reveals that the corrosion rate and the inhibition efficiency remain nearly constant when the poly-NDTHDC concentration was increased from 50 to 100 mg/L. For instance, the inhibition efficiencies of 50, 75, and 100 mg/L poly-NDTHDC are 80.0, 82.2, and 85.5% and the corrosion rates are 1.16, 1.03, and 0.83 mm/year, respectively. It suggests that the polymer film covered nearly all of the active centers when 50 mg/L was added such that

further addition had a minimal effect on the efficiency and the corrosion rate. Yaocheng et al.[19] recently gave a similar explanation.

As earlier mentioned, the larger number of binding sites in a single polymer molecule relative to its monomer makes polymers more effective as a metal corrosion inhibitor. The positive influence of polymerization on the inhibition performance of NDTHDC can be clearly seen in Figure 1. The least studied concentration of poly-NDTHDC performed far better than the highest studied concentration of NDTHDC. For instance, the corrosion rate and the inhibition efficiency of 10 mg/L poly-NDTHDC are 1.76 mm/year and 69.7%, respectively, whereas 100 mg/L NDTHDC afforded an inhibition efficiency of 43.9% and a corrosion rate of 3.25 mm/year. The protection efficiency achieved with 100 mg/L poly-NDTHDC (85.5%) is higher than the inhibition efficiency of 1000 mg/L NDTHDC (79.1%). It does mean that it is profitable in terms of cost and performance to use poly-NDTHDC instead of NDTHDC.

2.3. Electrochemical Studies.

2.3.1. Open-Circuit Potential (E_{ocp}) Studies.
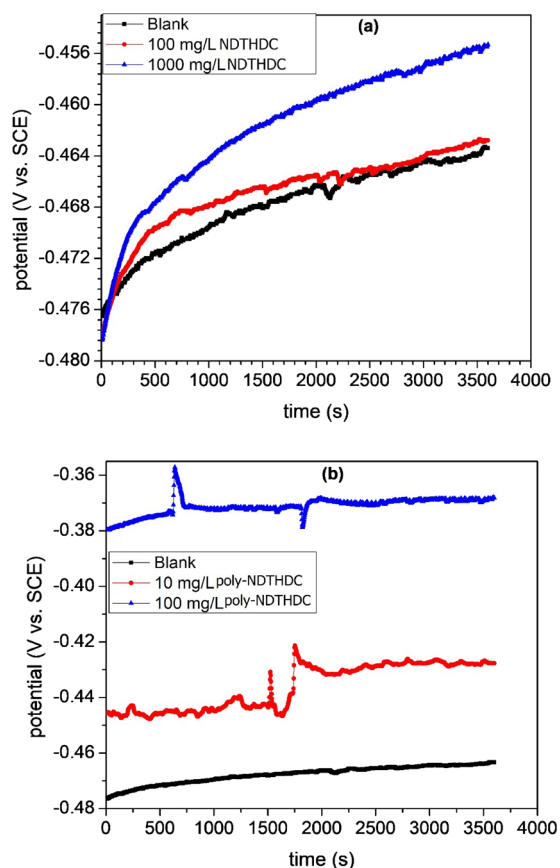
Figure 2 shows the variation of E_{ocp}

Figure 2. Variation of open-circuit potential (E_{ocp}) with time for API X60 steel in 15 wt % HCl solution in the absence and presence of (a) NDTHDC and (b) poly-NDTHDC at 25 °C.

with time for API X60 steel in 15 wt % HCl solution in the absence and presence of (a) NDTHDC and (b) poly-NDTHDC at 25 °C. In the blank solution (15 wt % HCl), the E_{ocp} begins at −476 mV vs SCE and progresses in a positive direction until a steady-state condition was reached. Such progression, according to authors,[20,21] is due to the premier corrosion process of the pre-exposure, air-formed

oxide layer, and the attack on the substrate surfaces. Compared to the E_{ocp} vs time graph of the blank, the E_{ocp} in the inhibited systems is shifted in the anodic direction. This indicates the preferential adsorption of NDTHDC and poly-NDTHDC on the anodic sites of the steel interface.[21] It is obvious from Figure 2b that poly-NDTHDC behaves more like an anodic-type inhibitor than NDTHDC (Figure 2a). Meanwhile, the displacement of the open-circuit potential by both NDTHDC and poly-NDTHDC is not up to the benchmark of +85 mV/Ref required for an anodic-type inhibitor;[22−24] hence, they are categorized as a mixed-type inhibitor. In both uninhibited and inhibited systems, the chosen 3600 s was sufficient for steady-state conditions to be reached.

2.3.2. Electrochemical Impedance Spectroscopy (EIS) Studies.

The EIS spectra recorded for API X60 steel in 15 wt % HCl solution in the absence and presence of (a, b) NDTHDC and (c, d) poly-NDTHDC at 25 °C are presented in Figure 3. Expectedly, the Nyquist graphs (Figure 3a,c) exhibit a single and depressed semicircle, which is a common feature of a solid electrode whose corrosion process is controlled by a charge-transfer mechanism.[22,25,26] In both the uninhibited and inhibited systems, the semicircles are similar and infer the same corrosion mechanism. However, the capacitive loops recorded in the inhibited systems are larger compared to the capacitive loop of the uninhibited system. This indicates a higher charge-transfer resistance of the working electrode in the inhibited systems than in the uninhibited system.[22,25,27] It demonstrates the presence of the protective film on the electrode surface probably due to the adsorption of NDTHDC or poly-NDTHDC molecules.[25,27]

The effect of concentration on the corrosion inhibition performance of the studied inhibitors is obvious in Figure 3. A larger semicircle is observed in systems inhibited with a higher concentration of NDTHDC or poly-NDTHDC (1000 mg/L NDTHDC or 100 mg/L poly-NDTHDC) relative to a lower concentration (100 mg/L NDTHDC or 10 mg/L poly-NDTHDC) (Figure 3a,c). More so, log/Z/ and phase angle are displayed for higher values by the higher concentration than the lower concentration (Figure 3b,d). All of these are reflective of the better inhibition performance of the higher concentration than the lower concentration. This could be explained on the premise that more inhibitor molecules were adsorbed and larger surface area covered upon addition of a higher concentration of NDTHDC or poly-NDTHDC to the corrosive system.[25]

The analysis of the EIS data was accomplished using a simple $R(QR)$ equivalent circuit. The diagram of the equivalent circuit can be found in our previous publication.[22] The selection of the equivalent circuit was informed by the monocular maxima of the Bode angle curves (Figure 3b,d) and the single-charge-transfer phenomenon as observed in Figure 3a,c. The equivalent circuit consists of a solution resistance (R_s), a charge-transfer resistance (R_{ct}), and a constant phase element (CPE), whose inclusion was necessitated by the depressed character exhibited by the Nyquist graphs (Figure 3a,c).[22,25−27] The impedance function of the CPE can be expressed according to eq 1[22,25]

$$Z_{CPE} = Y_0^{-1}(jw)^{-n} \tag{1}$$

where Y_0 is a CPE constant, n is a CPE exponent, j is an imaginary number, and w is the angular frequency. Normally, the mathematical coefficient n lies in the range $-1 \leq n \leq 1$.[21,28,29] The CPE would behave as an inductor if $n = -1$, a
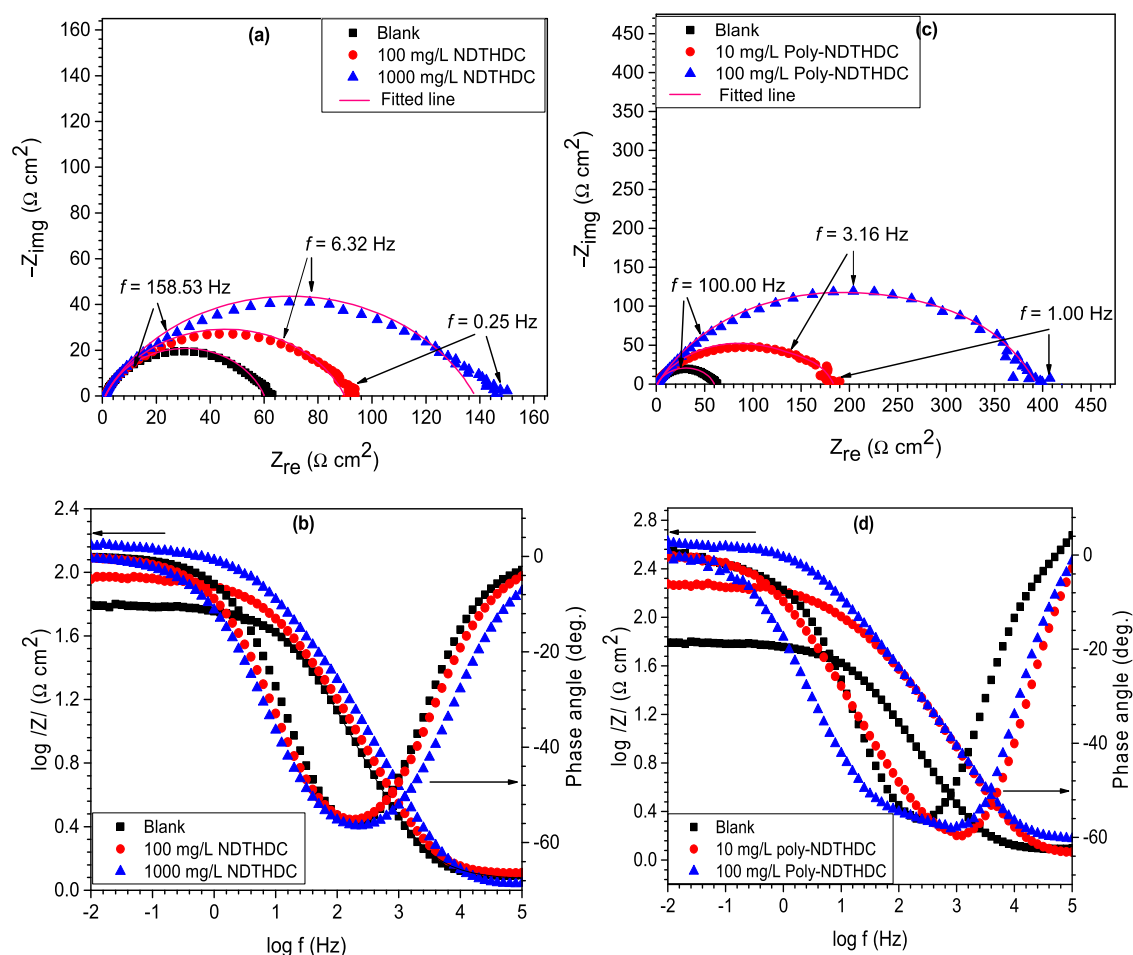
Figure 3. Electrochemical impedance spectra for API X60 steel in 15 wt % HCl solution in the absence and presence of (a, b) NDTHDC and (c, d) poly-NDTHDC at 25 °C.

Table 1. Impedance Parameters for API X60 Steel in 15 wt % HCl in the Presence and Absence of Selected Concentrations of NDTHDC and poly-NDTHDC at 25 °C

inhibitor	conc. (mg/L)	R_s (Ω cm^2)	CPE_{dl} Y_o ($\mu\Omega/(s^2$ cm^2))	n	R_{ct} (Ω cm^2)	C_{dl} (μF/cm^2)	η (%)	$\chi^2 \times 10^{-3}$
NDTHDC	0	1.17 ± 0.06	462.0	0.78	58.9 ± 2.95	0.57		1.77
	100	1.17 ± 0.06	533.5	0.74	88.8 ± 4.44	0.40	33.67 ± 1.68	2.67
	1000	0.95 ± 0.05	471.9	0.72	137.3 ± 6.87	0.24	57.10 ± 2.86	2.45
poly-NDTHDC	10	0.94 ± 0.05	349.8	0.72	174.5 ± 8.73	0.15	66.25 ± 3.31	7.35
	100	1.25 ± 0.06	269.7	0.71	388.1 ± 8.41	0.10	84.82 ± 4.24	4.35

resistor if $n = 0$, Warburg impedance if $n = 0.5$, and a capacitor if $n = 1$.[21,28,29] In addition, the value of n provides information on the roughness of the surface film.[21,28,29] A small value of n is indicative of a rough surface.[21,28,29]

The electrochemical impedance parameters obtained for the studied systems are given in Table 1. The value of the double-layer capacitance (C_{dl}), also given in the table, was calculated using eq 7, which is appropriate for this kind of nonideally polarized electrode where charge transfer primarily controls the corrosion process.[22,30] It is clear from the table that the corrosion resistance property of the steel electrode was enhanced upon the addition of inhibitors to the corrosive solution. For instance, the addition of 100 mg/L NDTHDC or 10 mg/L poly-NDTHDC to the acid solution increased the charge-transfer resistance of the electrode from the initial values of 58.9−88.8 and 174.5 Ω cm^2 and protected the surface

against corrosion by 33.67 and 66.25%, respectively. It means that the adsorbed inhibitor molecules replaced water molecules and other corrosive ions originally adsorbed on the electrode surface.[21,25,27,29] The smaller value of C_{dl} in the inhibited solutions compared to the value in the uninhibited solution also provides strong evidence to the claim of the formation of a protective film on the electrode surface. Furthermore, increase in the concentrations of NDTHDC and poly-NDTHDC to 1000 and 100 mg/L, respectively, further raised the charge-transfer resistances to 137.3 and 388.1 Ω cm^2 and inhibition efficiencies to 57.10 and 84.82% but decreased the C_{dl} values to 0.24 and 0.10 μF/cm^2, respectively. This infers that the adsorption of the inhibitor molecules reduced the capacitance through the increase in the double-layer thickness ($C_{dl} = \frac{\varepsilon_0 \varepsilon}{d}S$, where ε_0 is the permittivity of air, ε is the local dielectric

constant, d is the film thickness, and S is the electrode surface[26]). It is also important to point out the smaller values of C_{dl} in the systems inhibited with poly-NDTHDC than in systems protected with NDTHDC (Table 1). It provides strong evidence of the denser and thicker adsorbed film of poly-NDTHDC than NDTHDC and in extension the better inhibition by poly-NDTHDC than NDTHDC.

$$C_{dl} = Y_0^{1/n}\left(\frac{1}{R_s} + \frac{1}{R_{ct}}\right)^{(n-1)/n} \tag{2}$$

2.3.3. Potentiodynamic Polarization (PDP) Studies. The PDP curves for API X60 steel recorded in 15 wt % HCl solution in the absence and presence of (a) NDTHDC and (b) poly-NDTHDC at 25 °C are displayed in Figure 4. In the
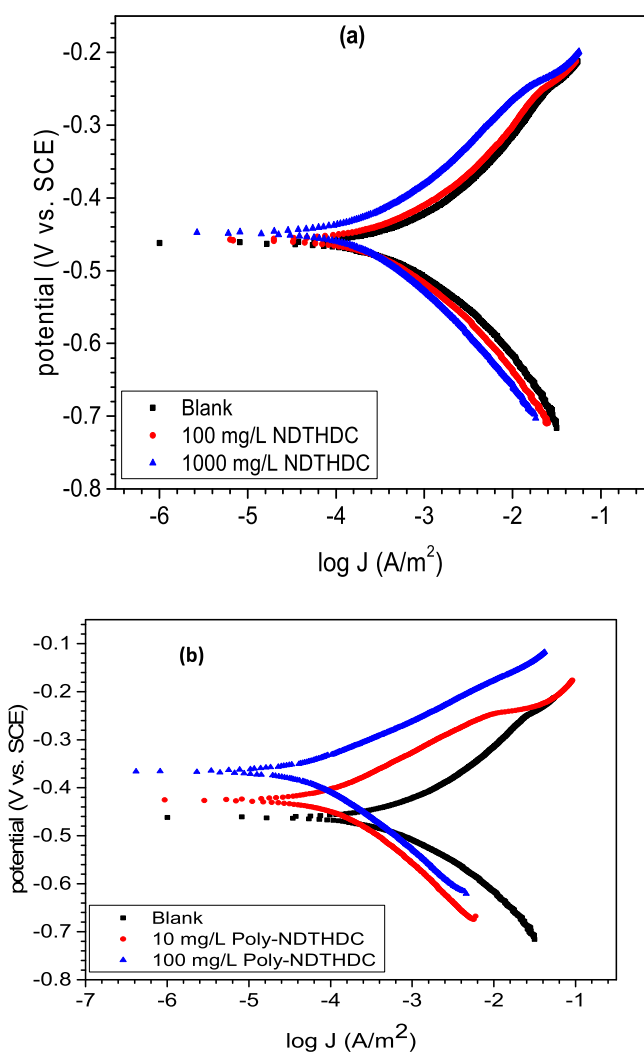

Figure 4. Potentiodynamic polarization curves for API X60 steel in 15 wt % HCl solution in the absence and presence of (a) NDTHDC and (b) poly-NDTHDC at 25 °C.

figure, the corrosion mitigation by NDTHDC and poly-NDTHDC, which is concentration-dependent, is demonstrated by the shifting of the current densities of the anodic ($2Fe_{(s)} \rightarrow 2Fe_{(aq)}^{2+} + 4e^-$) and cathodic ($2H_{(aq)}^+ + 2e^- \rightarrow H_{2(g)}$) branches to lower values. As indicated by the calculated values of C_{dl} (Table 1), the corrosion mitigation is due to the adsorption of the inhibitor molecules that apparently blocked

the steel surface active sites in the studied medium.[26,27] Furthermore, the corrosion potential (E_{corr}) is slightly shifted toward a more noble potential in both Figure 4a,b. The displacement is, however, more noticeable in Figure 4b than in Figure 4a. This is in excellent agreement with the E_{ocp} results (Figure 2) and supports the earlier proposition that the studied compounds inhibited both anodic and cathodic corrosion reactions but with a slightly higher effect on the anodic corrosion reaction.

The anodic and cathodic curves in Figure 4 were extrapolated to obtain polarization parameters such as E_{corr}, corrosion current density (J_{corr}), corrosion rate (v), and the anodic and cathodic Tafel slopes (β_a and β_c). The derived parameters are given in Table 2. The results show that the J_{corr}, v, and inhibition efficiency (η) variation is a function of the inhibitor concentration. It is clear that J_{corr} and v values decreased with increasing concentration of the inhibitor due to better protection by the higher concentration. The lowest v (0.70 mm/year) and best η (91.03%) were achieved with 100 mg/L poly-NDTHDC. The slight changes in the E_{corr} as well as the β_a and β_c values of the inhibited systems relative to the uninhibited ones further support the mixed-type behavior of the inhibitors.[20,21,27]

2.3.4. Linear Polarization (LPR) Studies. The corrosion of API X60 steel in 15 wt % HCl solution and the corrosion inhibition by NDTHDC and poly-NDTHDC at 25 °C was also studied using the linear polarization resistance (LPR) technique. The polarization resistance (R_p) values given in Table 2 were calculated using the slope of the potential vs current graphs (not shown) following eq 3.[31]

$$R_p = A\frac{dE}{di} \tag{3}$$

where A is the surface area of the working electrode and dE and di are the potential and current variations, respectively. The inhibition efficiency from this technique was also calculated using eq 4 but with R_{ct} replaced by the R_p value. The LPR result is in agreement with results from the other electrochemical techniques (Tables 1 and 2). As could be seen in Table 2, the polarization resistance of the steel electrode increased from 58.2 Ω cm^2 in the blank solution to 88.6 Ω cm^2 in 100 mg/L NDTHDC inhibited solution and corresponded to an inhibition efficiency of 34.3%. The R_p increased to 153.6 cm^2 upon increasing the monomer concentration to 1000 mg/L. For poly-NDTHDC inhibited systems, the presence of 10 mg/L raised the R_p to 197.5 Ω cm^2, and this ensures the protection of the metal surface by 70.5%. Further increment in the concentration of the polymer to 100 mg/L upgraded the inhibition efficiency to 85.9% by stepping up the polarization resistance to 413.4 Ω cm^2. This further demonstrates the effectiveness of poly-NDTHDC, in particular in suppressing the corrosion of low carbon steel in the acidizing solution.

2.4. Effect of Temperature on the Performance of NDTHDC and Poly-NDTHDC. Temperature is an important factor to consider when designing acidizing inhibitors because the recent depletion of shallower oil wells is driving drilling activities toward deeper wells with higher temperatures.[32] Unfortunately, a large number of organic compounds studied as acidizing corrosion inhibitors lost their inhibition performance drastically at temperatures higher than 60 °C.[3,22,33,34] In fact, only few such reports considered a temperature of up to 90 °C.[33,34]

Table 2. Polarization Parameters for API X60 Steel in 15 wt % HCl in the Presence and Absence of Selected Concentrations of NDTHDC and Poly-NDTHDC at 25 °C

inhibitor	conc. (mg/L)	PDP						LPR	
		$-E_{corr}$ (mV/SCE)	J_{corr} (μA/m^2)	β_a (mV/dec)	β_c (mV/dec)	ν (mm/year)	η (%)	R_p (Ω cm^2)	η (%)
NDTHDC	blank	461.4	664.6 ± 3.23	122.5	132.5	7.82 ± 0.39		58.2 ± 2.91	
	100	458.6	440.4 ± 2.02	109.2	129.9	5.18 ± 0.26	33.74 ± 1.69	88.6 ± 4.43	34.3 ± 1.72
	1000	449.5	304.6 ± 5.23	121.5	137.5	3.58 ± 0.18	54.17 ± 2.71	153.6 ± 7.68	62.1 ± 3.11
poly-NDTHDC	10	425.5	74.09 ± 3.70	87.90	106.0	0.87 ± 0.04	88.85 ± 4.44	197.5 ± 9.88	70.5 ± 3.53
	100	364.6	59.62 ± 2.98	84.60	133.6	0.70 ± 0.03	91.03 ± 4.55	413.4 ± 2.67	85.9 ± 3.30

To study the effect of temperature on the corrosion inhibition performance of NDTHDC and poly-NDTHDC in 15 wt % HCl solution, weight-loss experiments were undertaken at 25, 60, and 90 °C for 6 h. The concentrations of NDTHDC and poly-NDTHDC considered in these sets of experiments were 1000 and 100 mg/L, respectively. The results obtained are shown in Figure 5. Expectedly, the corrosion rate increases with the increase in temperature due to the increase in the average kinetic energy of the corrosive
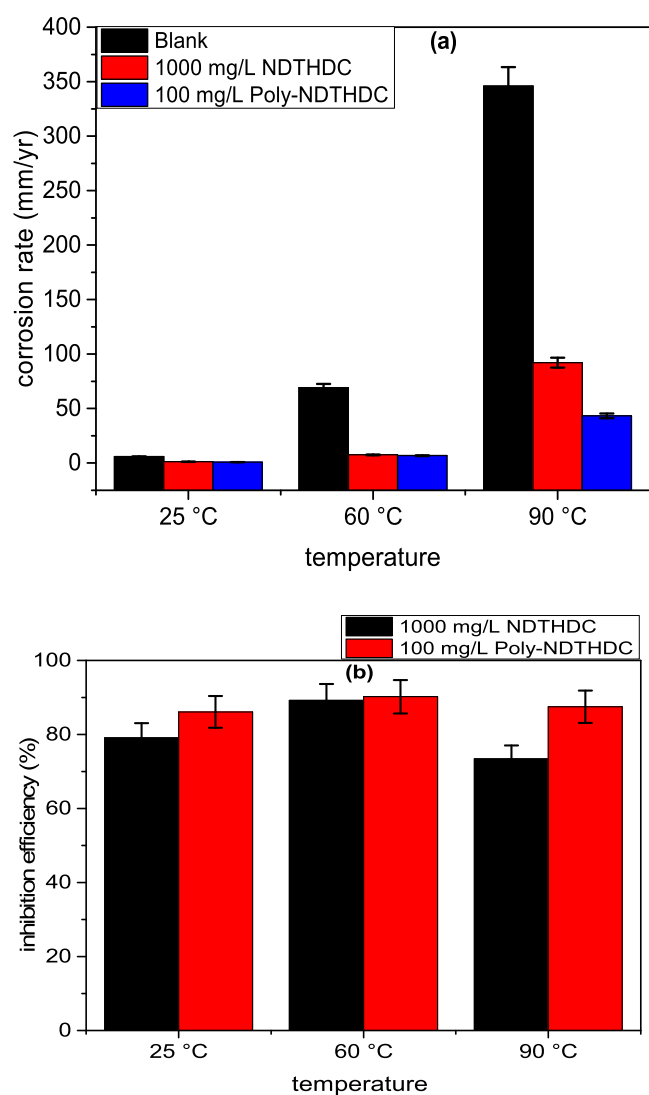
Figure 5. Comparative bar chart showing the effect of temperature on the (a) corrosion rate of API X60 steel and (b) inhibition efficiency of NDTHDC and poly-NDTHDC in 15 wt % HCl solution.

ions.[35] An astonishingly high corrosion rate of 346 mm/year was obtained in the blank acid solution at 90 °C. This shows that corrosion inhibitor technology is a necessity in the acidizing process. The presence of NDTHDC and poly-NDTHDC significantly reduced the corrosion rates to 92.1 and 43.4 mm/year, respectively. Inspection of Figure 5b reveals that the inhibition efficiency (η) of the additives increased with an increase in temperature up to 60 °C but slightly depreciated thereafter. For poly-NDTHDC, η increased from 86.1% at 25 °C to 90.2% at 60 °C but decreased to 87.5% at 90 °C. Similarly, for NDTHDC, η increased from 79.1% at 25 °C to 89.2% at 60 °C and then decreased to 73.4% at 90 °C. The observed increment in η between 25 and 60 °C is common with inhibitors that interact with the metal surface chemically.[13] The additives (NDTHDC and poly-NDTHDC) have the potential to interact chemically with the steel surface. The electron pair on the nitrogen heteroatom and the ring π-electrons in their structures (Scheme 1) can be engaged in a covalent type of bonding with the empty d-orbital of Fe.[13,36,37] The slight decrease in η observed between 60 and 90 °C may be due to the desorption of some of the adsorbed inhibitor films.[13] Worthy of pointing out is the effective inhibitive performance of poly-NDTHDC even at 90 °C (87.5%). This portrays poly-NDTHDC as a promising candidate for the formulation of an acidizing inhibitor cocktail. An organic inhibitor with inhibition efficiency of up to 70% at temperature ≥90 °C can be considered as a promising candidate.

2.5. Corrosion Inhibition by NDTHDC and Poly-NDTHDC under Hydrodynamic Conditions. Flow had been found to mostly boost the corrosion resistance of carbon steel in various corrosive media. For instance, Obot et al.[38] reported that the polarization resistance (R_p) of carbon steel in CO$_2$-saturated 3.5 wt % NaCl solution under the static condition was 145 ± 1 Ω cm^2 but 228 ± 2 Ω cm^2 under the hydrodynamic condition (1500 rpm). In a similar report,[39] it was found that the R_p of API X60 steel in NACE brine ID196 increased from 519 ± 4.8 Ω cm^2 under the static condition to 628 ± 2.8 Ω cm^2 at the 2000 rpm flow condition. Douadi et al.[40] also observed a steady decrease in the corrosion current density of mild steel in HCl solution from 0.4460 mA/cm^2 at the static condition to 0.3775 mA/cm^2 at 500 rpm rotation speed to 0.2592 mA/cm^2 at the 2000 rpm flow condition. It is believed that the enhanced corrosion resistance under the flow condition is due to the mass transport of corrosion products from the bulk solution to the metal surface.[38−40]

Flow condition has also been found to either improve or depreciate the corrosion inhibition performance of organic inhibitors. In the investigation by Obot et al.,[39] the inhibition performance of 7.68 mM 2-(2-pyridyl)benzimidazole against API X60 steel corrosion in NACE ID196 brine solution was

found to improve from 67.3% at the static condition to 95.2% at the 1500 rpm flow condition but decreased to 90.7% when the rotation speed was increased to 2000 rpm. We also recently reported[22] that the charge-transfer resistance of a low carbon steel in a 15 wt % HCl solution inhibited with 400 mg/L 2-heptadecyl-1-[2-(octadecanoylamino)ethyl]-2-imidazoline increased from 80.93 Ω cm^2 at 0 rpm to 194.20 Ω cm^2 at 1000 rpm but decreased drastically to 58.04 Ω cm^2 at 1500 rpm. The improvement in the corrosion inhibition performance of organic inhibitors under hydrodynamic conditions is often attributed to the mass transport of the inhibitor molecules from the bulk solution to the substrate surface.[22,38,39] The poor performance at a high flow rate as was observed by Solomon et al.[22] is often linked to shear stress believed to cause the detachment of adsorbed inhibitor species from the substrate surface.[22,38,39]

To study the influence of flow on the dissolution behavior of the API X60 steel in 15 wt % HCl solution and on the corrosion inhibition performance of NDTHDC and poly-NDTHDC, experiments were undertaken under the hydro-dynamic condition at 60 °C utilizing the rotation speeds of 500, 1000, and 1500 rpm (Figure 6). The temperature (60 °C) was chosen since the inhibition efficiency of the additives was maximum at this temperature (Figure 5). At 0 rpm, the corrosion rate of the studied metal substrate in the corrosive HCl solution is 69.2 mm/year (Figure 5a) but decreased to 32.0 mm/year at 500 rpm (Figure 6a). This is in excellent agreement with the findings of other researchers.[22,38−40] It was reported that hydrodynamic flow facilitates the presence of dissolved oxygen and H$^+$ ions on the substrate surface and consequently promotes oxide formation on the surface.[41] The observed decrease in the corrosion rate at higher velocities could be due to the above reasons. The results in Figure 6b indicate that the corrosion inhibition performance of NDTHDC and poly-NDTHDC improves under the hydro-dynamic condition relative to the static condition, and 1000 rpm seems to be the most favorable flow condition. The inhibition efficiencies of 89.2 and 90.2% for NDTHDC and poly-NDTHDC, respectively, at 0 rpm increased to 90.9 and 91.6% at 1000 rpm. Further increase in rotation speed to 1500 rpm resulted in a decline in the inhibition efficiency of the additives. The reasons for these observations may not be far from the hypotheses of mass movement of inhibitor molecules to the metal surface and the detachment at a high flow rate due to shear stress.[22,38,39]

2.6. Thermal and Chemical Stability Studies. The thermal and chemical stability of a surface inhibitor film is very vital for its applications. As earlier mentioned, the acidizing process is carried out utilizing concentrated acids (15−28 wt %) at temperatures exceeding 90 °C.[1] Therefore, the organic inhibitors are expected to be thermally and chemically stable to provide the required effective protection under these harsh conditions.[42] The comparative thermogravimetric analysis (TGA) graphs for pure poly-NDTHDC and recovered poly-NDTHDC films after being heated in a 15 wt % HCl solution at 90 °C for 12 h are shown in Figure 7a. It is obvious that the polymer before and after heating is stable up to 214 °C. Nevertheless, the results of the analysis of the region 30−214 °C reveal 6.71 and 17.12% losses in the weights of the unheated and heated poly-NDTHDC, respectively. The weight loss occurred majorly at 100−170 °C and could be attributed to the loss of moisture and dopants.[42] It should be pointed out that, at 400 °C, about 20% of the polymer was still
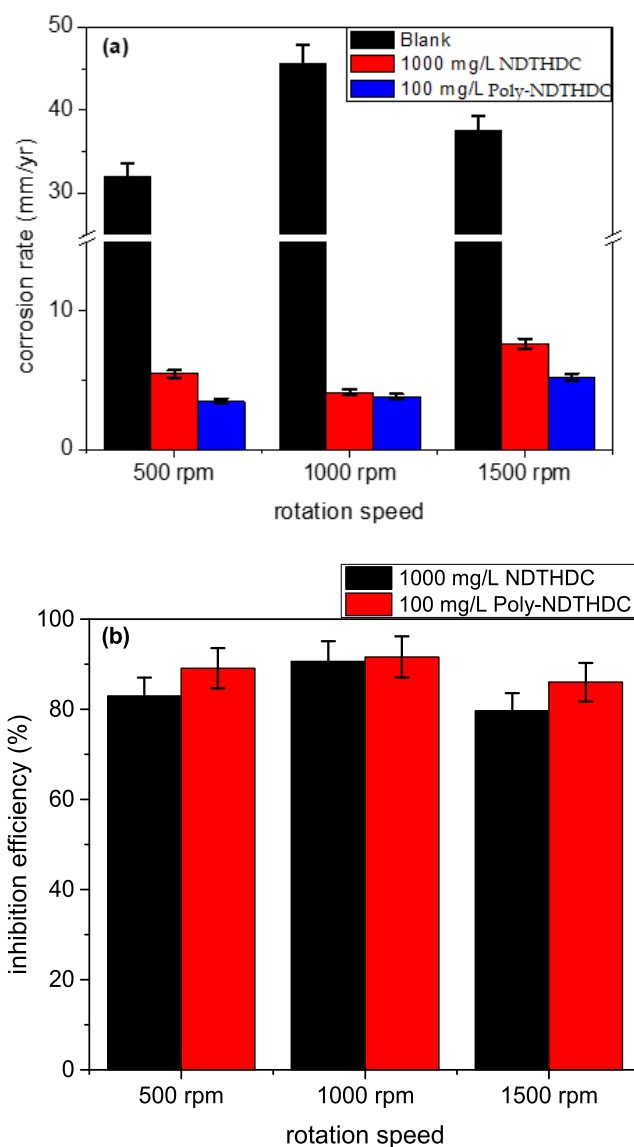

Figure 6. Comparative bar chart showing the effect of flow on the (a) corrosion rate of API X60 steel and (b) inhibition efficiency of NDTHDC and poly-NDTHDC in 15 wt % HCl solution at 60 °C.

undecomposed. These results show that poly-NDTHDC is stable in 15 wt % HCl solution and is thermally stable up to 214 °C.

It is expected that the functional groups in an inhibitor molecule remain intact in the environment of application. That is, they should not undergo significant changes if the inhibitor is stable in the environment of usage. Figure 7b shows the FTIR curves of poly-NDTHDC before and after heating. In the pure poly-NDTHDC (before heating) spectrum, peaks are found at 3382.85, 2935.15, 2874.88, 2580.13, 2360.30, 2340.70, 1673.13, 1460.12, 1385.67, 1270.12, 1152.65, 1041.31, 961.41, 851.88, 754.76, and 607.40 cm^{-1}. The peak at 3382.85 cm^{-1} is assigned to the N−H of the tertiary amine.[22] The peaks at 2935.15 and 2874.88 cm^{-1} are associated with the C−H in CH$_3$ and CH$_2$, respectively, stretching.[22,37] The peaks at 1673.13 cm^{-1} are linked to C=N stretching,[43] while the peaks at 1385.67 and 1041.31 cm^{-1} are assigned to the ring and tertiary amine C−N stretching, respectively.[43] The stretching of the aromatic C−C group is associated with the peak at 1460.12 cm^{-1}.[44] Compared with
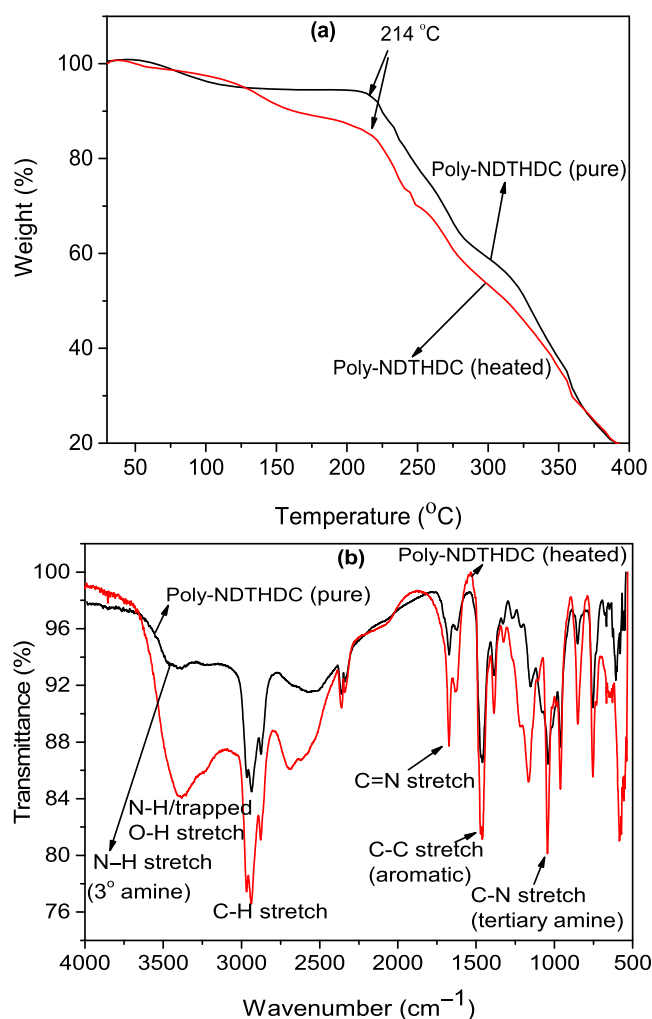
Figure 7. Comparative (a) TGA and (b) FTIR spectra of pure poly-NDTHDC and poly-NDTHDC recovered from 15 wt % HCl solution after being heated at 90 °C for 12 h.

the FTIR spectrum of the heated poly-NDTHDC, all of the above-listed peaks are intact, confirming the TGA results that poly-NDTHDC is stable in 15 wt % HCl solution and also thermally stable. The broadness of the peaks at around 3380 and 2680 cm^{-1} may be due to the entrapped water molecules.

2.7. Surface Characterization Studies. *2.7.1. SEM and Energy-Dispersive X-ray Spectroscopy (EDAX) Studies.* The SEM micrographs and the EDAX spectra of the API X60 steel sample surface (a, b) before immersion and after immersing in 15 wt % HCl solution containing (c, d) no inhibitor, (e, f) 1000 mg/L NDTHDC, and (g, h) 100 mg/L poly-NDTHDC for 6 h at 90 °C are shown in Figure 8. The SEM micrograph of the abraded surface (Figure 8a) reveals a smooth morphology; an intense Fe peak is seen in the corresponding EDAX spectrum (Figure 8b). The sample corroded seriously in 15 wt % HCl solution as revealed by the rough morphology of the surface in Figure 8c. Heaps of porous corrosion products can be visibly seen on the surface in Figure 8c. Previous studies[13,45,46] identified the corrosion products as a non-stoichiometric mixture of chlorides, carbonates, oxides, and oxide-hydroxides of iron. The EDAX result in Figure 8d is in agreement with previous findings. The presence of Cl (12.3%), O (9.6%), and C (8.4%) in Figure 8d provides experimental

evidence that the corrosion products are a mixture of chlorides, oxides/oxide-hydroxides, and carbonates.

The film deposited on the steel surface exposed to 15 wt % HCl solution containing 1000 mg/L NDTHDC is more rigid compared to the one on the surface of Figure 8c. It means that the adsorbed NDTHDC film withstood the aggressive conditions (i.e., 90 °C and highly corrosive acid solution) and better protected the steel surface than the porous corrosion products. Meanwhile, the EDAX results in Figure 8f indicate that the adsorbed inhibitor molecules (N band in Figure 8f is a proof of NDTHDC adsorption) were incorporated in the corrosion product mixture. For instance, the O, C, and Cl bands are still intact in Figure 8f although the amount present was reduced.

Obviously, poly-NDTHDC is effective as a corrosion inhibitor for API X60 steel in 15 wt % HCl solution. As could be clearly seen in Figure 8g, the steel surface was highly protected. The surface morphology is comparable to the morphology of the abraded specimen (Figure 8a). The corresponding EDAX spectrum (Figure 8h) reveals that there was a significant decrease in the weight percentage of chloride ions on the surface inhibited by poly-NDTHDC. The chloride content decreased from 12.3% in Figure 8b to 0.4% in Figure 8h.

2.7.2. AFM Studies. Figure 9 presents the AFM images and the associated surface roughness characteristics of the API X60 steel sample surface (a) before immersion and after immersing in 15 wt % HCl solution containing (b) no inhibitor, (c) 1000 mg/L NDTHDC, and (d) 100 mg/L poly-NDTHDC for 6 h at 90 °C. The steel sample surface immersed in the corrodent is rougher (Figure 9b) compared to the abraded surface (Figure 9a) due to corrosion. Compared with the values of the surface roughness parameters in the table inserted in Figure 9a, there is a significant increase in the values of the parameters in the table inserted in Figure 9b. The maximum band height (R_p), maximum valley depth (R_v), and the largest band-to-valley height (R_t) increased by 86, 80, and 83%, respectively. This shows that the steel sample severely corroded in the HCl solution. By comparing the surfaces in Figure 9c,d to the surface in Figure 9b, it is very clear that the additives protected the steel surface from corrosion. The surfaces are smoother compared to the surface in Figure 9b, and all of the values of the surface roughness parameters in the inserted tables in Figure 9c,d are smaller than the values in the table inserted in Figure 9b. Interestingly, except for the R_{ku} value, all of the values of the roughness parameters in the table inserted in Figure 9d are smaller than 0.1 μm and clearly demonstrate the excellent protection offered by poly-NDTHDC to the steel surface. The AFM results are in good agreement with the SEM (Figure 8g) and the experimental results (Tables 1 and 2).

2.7.3. Contact Angle Studies. The formation of an NDTHDC- or poly-NDTHDC-based hydrophobic film on the API X60 steel sample surface immersed in 15 wt % HCl solution inhibited with NDTHDC or poly-NDTHDC was also verified by water contact angle measurements. Figure 10 shows the water droplet contact angle images on API X60 steel surfaces before (a) immersion and after immersion in (b) 15 wt % HCl solution devoid of an inhibitor, (c) 15 wt % HCl solution containing 1000 mg/L NDTHDC, and (d) 15 wt % HCl solution containing 100 mg/L poly-NDTHDC for 6 h at 90 °C. The contact angle of the reference surface (Figure 10a) is 89.9°. Upon immersion in the corrodent for 6 h at 90 °C, the contact angle decreased to 15.4° in agreement with reports
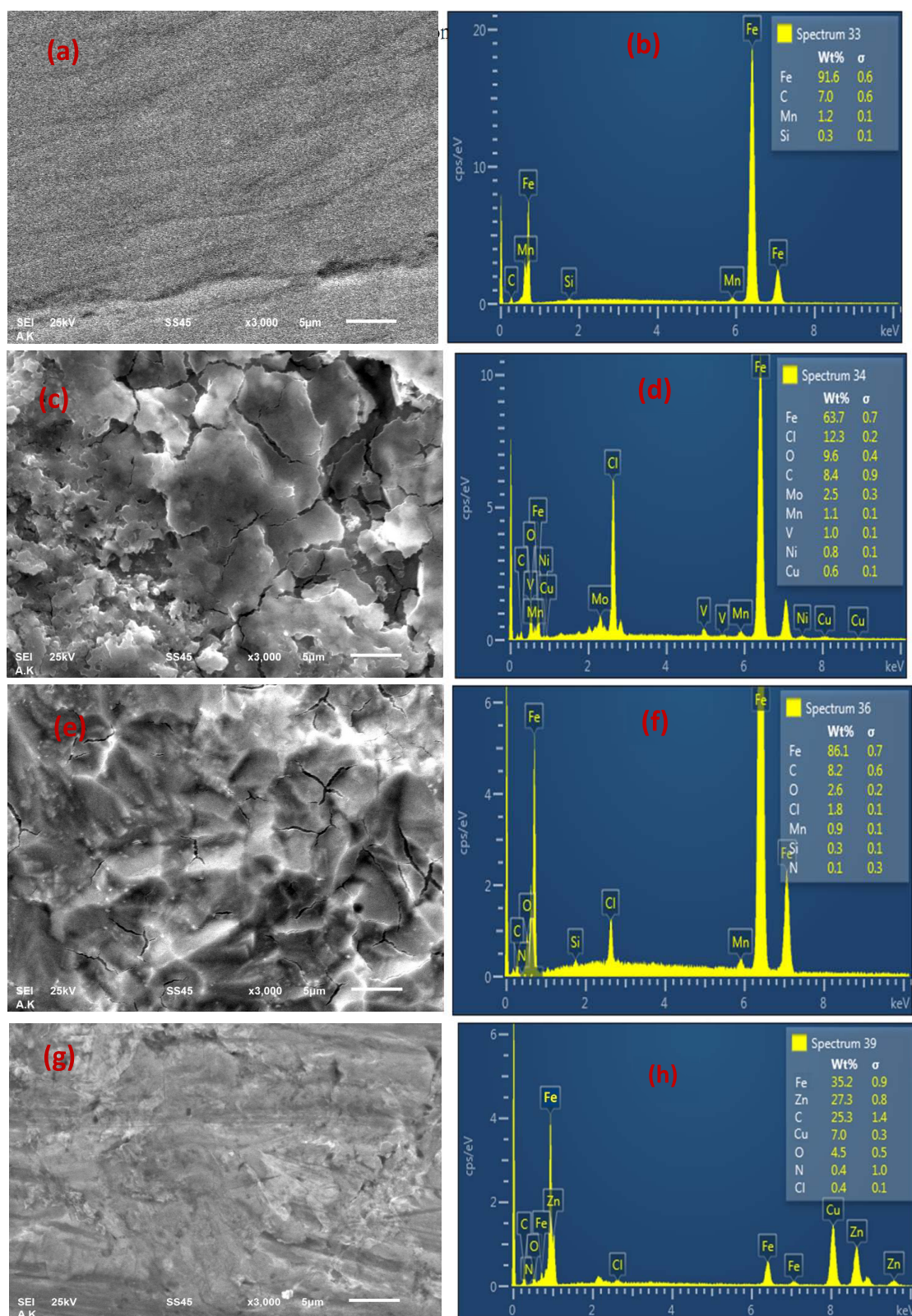
Figure 8. SEM pictures and EDAX spectra showing the surface morphology and composition of the API X60 steel sample surface (a, b) before immersion and after immersing in 15 wt % HCl solution containing (c, d) no inhibitor, (e, f) 1000 mg/L NDTHDC, and (g, h) 100 mg/L poly-NDTHDC for 6 h at 90 °C.

from other authors[47−50] and indicates a higher hydrophilic surface caused by increased surface roughness[47−49] and the formation of polar inorganic corrosion products on the steel surface that enhanced surface wettability.[47−50] Compared with

the contact angle on the API X60 steel surface immersed in 15 wt % HCl solution containing NDTHDC and poly-NDTHDC, the contact angles on the inhibited surfaces increased to 24.6° (Figure 10c) and 34.3° (Figure 10d), respectively. It indicates
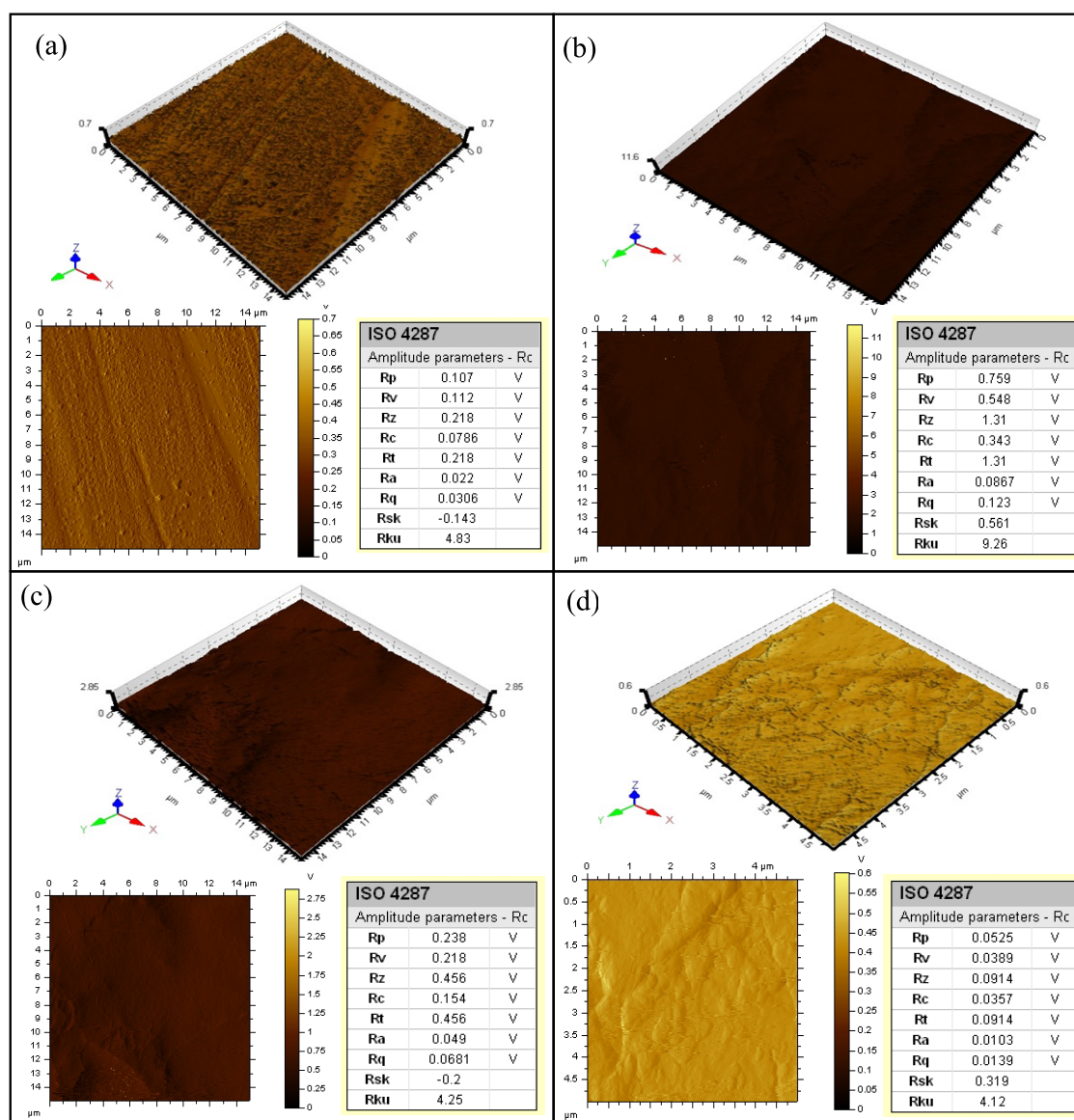
Figure 9. AFM images and associated surface roughness parameters for the API X60 steel sample (a) before immersion and after immersing in 15 wt % HCl solution containing (b) no inhibitor, (c) 1000 mg/L NDTHDC, and (d) 100 mg/L poly-NDTHDC for 6 h at 90 °C.

that the surface roughness and corrosion products reduced in the inhibited surfaces, as evidenced in the AFM results (Figure 9c,d). It is observed that the contact angle on the poly-NDTHDC inhibited surface is 9.7° higher than that on the NDTHDC inhibited surface, indicating an increase in the hydrophobicity of the surface and conforming to other experimental results (Table 1 and 2 and Figure 5) that the inhibition property of poly-NDTHDC is better than that of NDTHDC.

2.8. Possible Inhibition Mechanism by NDTHDC and Poly-NDTHDC. Generally, organic inhibitors inhibit metal corrosion through the adsorption mechanism.[13,21,39] This involves the substitution of adsorbed water molecules and other corrosive species on the metal surface by adsorbed inhibitor molecules.[13,21,39] Several factors affect the inhibition process.[13,21,39] Most importantly, the metal surface charge and the state of an organic molecule in a corrosive environment have a profound influence on the adsorption process.[51] Research studies[13,21,22,42] have shown that the surface of carbon steel in HCl solution carries a net positive charge and

chloride ions preferentially adsorbed on the surface. The specific adsorption creates excess electrons on the surface, and this allows cationic species to be adsorbed on the surface.[13,21,22,42] Unarguably, NDTHDC and poly-NDTHDC would be protonated in 15 wt % HCl solution and could be electrostatically dragged onto the metal surface (physisorption). The nitrogen heteroatom could be freed on the surface. The electron pair in addition to π-electrons in the inhibitor molecules (see Scheme 1) could form coordination and back-donating bonds with the empty d-orbital of iron through donor−acceptor interaction (chemisorption). The proposed inhibition mechanism is illustrated in Figure 11.

Meanwhile, the results of the variation of inhibition efficiency with temperature presented in Figure 5b suggest a mixed adsorption mechanism (i.e., both physical and chemical adsorption). According to Lgaz et al.,[52] physical adsorption is the first step before chemical adsorption. To ascertain which of these two kinds of interactions was prevalent, UV−vis experiments were performed. Figure 12 shows the UV−visible spectra of NDTHDC and poly-NDTHDC in 15 wt % HCl
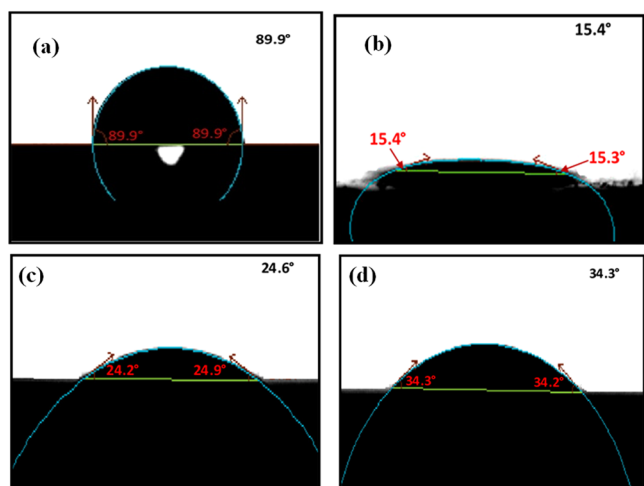
Figure 10. Water droplet contact angle on API X60 steel surfaces after (a) mechanical abrasion, (b) immersed in 15 wt % HCl solution devoid of inhibitor, (c) immersed in 15 wt % HCl solution containing 1000 mg/L NDTHDC, and (d) immersed in 15 wt % HCl solution containing 100 mg/L poly-NDTHDC for 6 h at 90 °C.
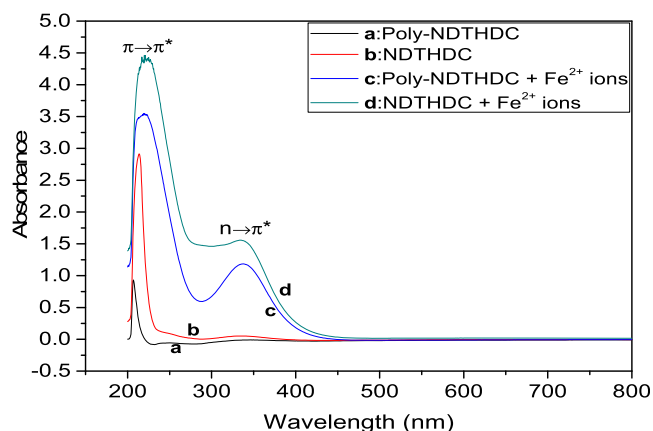

Figure 12. UV−visible spectra of NDTHDC and poly-NDTHDC in 15 wt % HCl solution (a, b) before and (c, d) after introduction of the API X60 steel sample for 6 h at 90 °C.

solution (a, b) before and (c, d) after the introduction of the API X60 steel sample for 6 h at 90 °C. The UV−vis spectra of the NDTHDC and poly-NDTHDC solution exhibit only the characteristic $\pi \rightarrow \pi^*$ band at around 200 nm.[53] In the UV−vis spectra of the NDTHDC and poly-NDTHDC + Fe²⁺ ion solutions, a new band at about 341 nm is observed, which arose due to the complex formation between Fe and the additives.[21] This outcome indicates that the dominant adsorption mechanism of NDTHDC and poly-NDTHDC on the API X60 steel surface in 15 wt % HCl solution is chemisorption.

3. CONCLUSIONS

During well acidizing, corrosion of tube materials and facilities is a serious challenge.[3,33] Corrosion inhibition technology is an effective and low-cost corrosion mitigation approach.[4,51] Because of environmental litigations, efforts have been intensified to develop eco-friendly corrosion inhibitors.[44,52,53] Herein, a novel dicationic monomer (NDTHDC) and its polymer (poly-NDTHDC) have been studied as corrosion inhibitors for API X60 steel in 15 wt % HCl solution at a temperature ranging from 25 to 90 °C. Experimental results show that although both NDTHDC and poly-NDTHDC
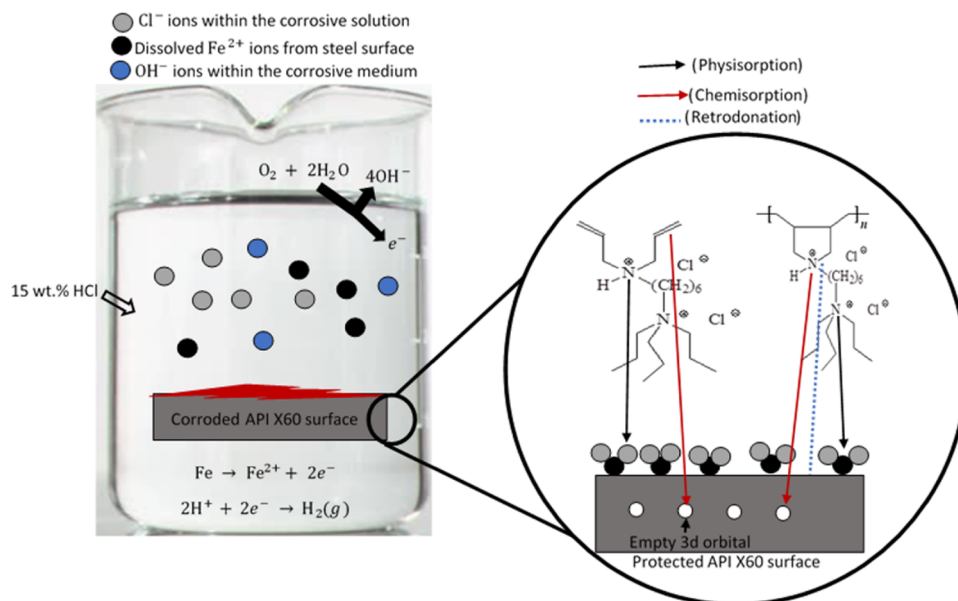

Figure 11. Proposed API X60 carbon steel corrosion inhibition mechanism in 15 wt % HCl solution by NDTHDC and its polymer (poly-NDTHDC). The presence of NDTHDC or poly-NDTHDC films on the carbon steel surface limited the penetration of the corrosive ions to the carbon steel surface and by so doing protected the surface. The formation of the protective surface film by NDTHDC or poly-NDTHDC must have been accomplished via N heteroatoms and the unsaturated double bond (in the case of NDTHDC). The electrostatic attraction between the protonated NDTHDC or poly-NDTHDC molecules and the preadsorbed counter Cl⁻ ions on the carbon steel surface resulted in the physical adsorption of the inhibitor molecules on the metal surface. Donor−acceptor interactions could occur between these chemical groups and the vacant orbital of Fe. There is also a possibility of retrodonation with any antibonding orbitals.

possess inhibiting effect toward the API X60 steel in the studied corrosive medium, poly-NDTHDC is by far a better inhibitor. From the weight-loss technique, 1000 mg/L NDTHDC protected the metal surface at 25 °C by 79.1%, whereas 100 mg/L poly-NDTHDC inhibited the substrate corrosion by 86.1%. An increase in temperature from 25 to 60 °C is found to cause an increase in the inhibition efficiency of the studied inhibitors. The inhibition efficiency depreciates slightly at a temperature of 90 °C. The inhibition efficiency of 100 mg/L poly-NDTHDC increased from 86.1% at 25 °C to 90.2% at 60 °C but decreased to 87.5% at 90 °C. Both NDTHDC and poly-NDTHDC, according to the potentiodynamic polarization results, behave as a mixed-type corrosion inhibitor. NDTHDC and poly-NDTHDC perform better under hydrodynamic conditions than static conditions. Their best performance is at a flow condition of 500−1000 rpm. The SEM and AFM results are in good agreement with other experimental results and clearly show that poly-NDTHDC is highly effective in retarding the corrosion of API X60 steel in 15 wt % HCl solution even at 90 °C. TGA and FTIR results show that poly-NDTHDC before and after the addition to the corrodent is stable. The polymer is thermally stable up to 214 °C. The FTIR results reveal that the functional groups in poly-NDTHDC are intact when the polymer is added to the HCl solution and heated at 90 °C for 12 h. The mechanism of chemisorption is proposed for the interaction of both NDTHDC and poly-NDTHDC with the steel surface, and the UV−vis results confirmed complex formation. Poly-NDTHDC is a promising candidate for the formulation of an acidizing inhibitor.

4. MATERIALS AND METHODS

4.1. Materials, Chemicals, and Corrodent.
The API X60 pipe from which samples used in this work were made from was obtained from the oil and gas industry in Saudi Arabia. The elemental composition of the X60 steel is as given in Onyeachu et al.,[39] and the sample pretreatment process was as detailed in the ASTM G1-03.[54] The sample surfaces were abraded to a final 800-grit size using silicon carbide paper.

The chemicals used for the synthesis of the studied inhibitors were procured from Merck Schuchardt OHG and include diallylamine (99%; CAS-No: 124-02-7), 1,6-dibromohexane (96%; CAS-No: 629-03-8), 2,2′-azobis(2-methylpropionamidine)dihydrochloride (AMPD) (97%; CAS-No: 2997-92-4), and tripropyl amine. They were used as purchased without further purification.

The corrosive medium was 15 wt % HCl solution prepared by diluting concentrated hydrochloric acid (37%; purchased from Merck) with distilled water.

4.2. Synthesis. 4.2.1. Synthesis of Bis-Ammonium Salt 5.
First, a bromide salt **3** was prepared following the literature procedure.[13,14] Second, a mixture of bromide salt **3** (81% purity, 19.1 g, 40 mmol) and diallylamine **4** (13.6 g, 150 mmol) in acetonitrile (50 mL) was heated under N_2 in an oil bath at 95 °C for 20 h. The reaction mixture was then treated with water (25 mL) containing NaOH (1.6 g, 40 mmol). After the removal of acetonitrile and excess diallylamine, the residual mixture was treated with concentrated HCl (10 mL) and NaCl (30 g) and washed with ether (3 × 20 mL). The aqueous layer was freeze-dried, and the residue was thoroughly mixed with a liberal excess of hot acetone and filtered to remove NaCl. The filtrate was concentrated to obtain N^1,N^1-diallyl-N^6,N^6,N^6-tripropylhexane-1,6-diaminium chloride (NDTHDC) as a

yellow liquid (15.0 g, 95%). (Found: C, 63.1; H, 11.4; N, 6.8%. $C_{21}H_{44}Cl_2N_2$ requires C, 63.78; H, 11.21; N, 7.08%); $\nu_{max.}$ (neat) 3450, 2971, 2875, 1628, 1471, 1385, 1049, 1001, 955, 852, and 756 cm^{-1}. δ_H (D$_2$O): 0.78 (9H, t, J 7.0 Hz), 1.24 (m, 10H), 1.37 (6H, m), 3.00 (8H, m), 3.63 (4H, d, J 6.8 Hz), 5.46 (4H, m), 5.76 (2H, m); δ_C (D$_2$O): 10.8, 15.7, 21.8, 24.0, 26.0, 31.2, 52.7, 55.5, 58.9, 60.7, 126.4 ($\underline{C}H=$), 127.3 ($\underline{C}H_2=$). The DEPT 135 NMR spectrum confirmed the ^{13}C assignments.

4.2.2. Polymerization of NDTHDC to Obtain Poly-NDTHDC.
A solution of NDTHDC (8.5 g, 70 wt %, 21.5 mmol) in water (3.65 g, 30 wt %) containing initiator 2,2′-azobis(2-methylpropionamidine) dihydrochloride (AMPD) (200 mg) was stirred under N_2 at 95 °C for 24 h. After further addition of the initiator (150 mg), the mixture was stirred at 95 °C for 24 h. The thick reaction mixture was dialyzed against distilled water and freeze-dried to obtain poly(N^1,N^1-diallyl-N^6,N^6,N^6-tripropylhexane-1,6-diaminium chloride) (poly-NDTHDC) (6.0 g, 71%). (Found: C, 63.4; H, 11.5; N, 6.9%. $C_{21}H_{44}Cl_2N_2$ requires C, 63.78; H, 11.21; N, 7.08%); ν_{max} (KBr) 3440, 2964, 2717, 1633, 1472, 1387, 1126, 1047, 964, 854, 758, and 620 cm^{-1}.

4.2.3. Characterization of NDTHDC and Poly-NDTHDC.
Elemental analysis was carried out on a EuroVector Elemental Analyzer Model EA3000 (Milan, Italy). ^1H and ^{13}C NMR spectra of the NDTHDC and poly-NDTHDC were measured in D$_2$O using the HOD signal at δ 4.65 ppm and dioxan 67.8 ppm as internal standards, respectively, on a Brucker 400 MHz spectrometer (Germany).

4.3. Corrosion Studies. 4.3.1. Weight-Loss Measurements.
The standard procedure for immersion testing as detailed in NACE TM0169/G31[55] was followed in these sets of experiments. The weight-loss tests were performed under static and hydrodynamic conditions. Reaction bottles (150 mL capacity) were filled with 100 mL of test solutions (15 wt % HCl solution with and without different concentrations of inhibitor). They were placed in a Thermo Scientific precision water bath maintained at studied temperatures (25, 60, and 90 °C). The prepared API X60 steel specimens (2.97 cm × 2.86 cm × 1.10 cm; surface area = 30 cm^2) in triplicate were freely suspended in the test medium for 6 h. The concentrations of NDTHDC studied were 100, 250, 500, 750, and 1000 mg/L, while those of poly-NDTHDC were 10, 25, 50, 75, and 100 mg/L. After 6 h of immersion, the specimens were removed and subjected to the post-treatment procedures outlined in the ASTM standard G1-03.[54] Hydrodynamic experiments were conducted at rotation speeds of 500, 1000, and 1500 rpm achieved by placing the reaction bottles on a programmable stirring hot plate (model HS 65). The corrosion rate (v) was calculated using the average weight loss (g) following the equation[54]

$$v(\text{mm/year}) = \frac{87\,600 \times \overline{WL}}{\rho A \text{T}} \quad (4)$$

where $\overline{WL}$ is the average weight loss (g), ρ is the density of the sample (g/cm^3), T is the immersion time (6 h), and A is the surface area of the sample (30 cm^2). The surface area was calculated using eq 5. The protection efficiency (η_{WL}) of NDTHDC and poly-NDTHDC was computed using eq 6.

$$A = 2(wl + dl + dw) \quad (5)$$

where A is the area (cm^2), w is the width (cm), d is the thickness (cm), and l is the length (cm).

$$\%\eta_{\text{WL}} = \frac{W_0 - W}{W_0} \times 100 \qquad (6)$$

where W_0 and W are the average weight losses of the specimens in 15 wt % HCl solution without and with the inhibitor, respectively.

4.3.2. Electrochemical Measurements. All electrochemical experiments were performed in a three-electrode cell including an API X60 steel sample (working electrode), a graphite rod (auxiliary electrode), and a $\text{Ag}_{(s)}|\text{AgCl}_{(s)}|\text{sat.Cl}^-_{(aq.)}$ electrode (reference electrode). Experiments were performed under static conditions at 25 °C. Before performing electrochemical impedance spectroscopy (EIS) tests, the open-circuit potential (E_{ocp}) was monitored for 3600 s. The EIS tests were carried out at a frequency range of 100 000−0.01 Hz with a perturbation of 10 mV peak to peak. Linear polarization resistance (LPR) measurements were carried out utilizing 0.125 mV/s as the scan rate from −10 to +10 mV vs E_{ocp}. The potentiodynamic polarization (PDP) curves were recorded at the potential of ±250 mV vs E_{ocp} with a sweep rate of 0.2 mV/s. Gamry Echem Analyst was used for the analysis of the EIS impedances, LPR, and PDP curves. The protection efficiencies of NDTHDC and poly-NDTHDC from EIS and PDP techniques were calculated using eqs 7 and 8, respectively. Equation 6 was also used for the computation of inhibition efficiency from LPR measurements but with R_{ct} replaced with R_{p} (polarization resistance).

$$\%\eta_{\text{EIS}} = \left(1 - \frac{R_{\text{ct(blank)}}}{R_{\text{ct(inh)}}}\right) \times 100 \qquad (7)$$

$$\%\eta_{\text{PDP}} = \left(1 - \frac{J_{\text{corr(inh)}}}{J_{\text{corr(blank)}}}\right) \times 100 \qquad (8)$$

where $J_{\text{corr (blank)}}$ and $R_{\text{ct (blank)}}$ are the corrosion current density and the charge-transfer resistance, respectively, recorded in the uninhibited acid solution; and $J_{\text{corr(inh)}}$ and $R_{\text{ct(inh)}}$ are the corrosion current density and the charge-transfer resistance recorded in the acid solution containing the studied inhibitor, respectively.

4.3.3. Surface, Solution, and Thermal Analyses. After 6 h of immersion in a 15 wt % HCl solution without and with 1000 mg/L NDTHDC or 100 mg/L poly-NDTHDC at 90 °C, the corrosion products and/or adsorbed inhibitor films on the API X60 steel surface were carefully scrapped and subjected to Fourier transform infrared spectroscopy (FTIR) analysis. The experiments were conducted in the attenuated total reflectance (ATR) mode within the wavenumber range of 4000−500 cm^{-1} at a resolution of 4 cm^{-1} with the help of a PerkinElmer Version 10.03.05 FTIR spectrometer.

The surface morphology of the corroded steel after 6 h of immersion in 15 wt % HCl solution without and with 1000 mg/L NDTHDC or 100 mg/L poly-NDTHDC at 90 °C was observed using a scanning electron microscope (SEM), JEOL JSM-6610 LV model, coupled to energy-dispersive X-ray spectroscopy (EDAX) for chemical composition determination.

To obtain information on the roughness characteristics of the steel surface before and after corrosion, atomic force microscopy (AFM) images were obtained using a 5420 atomic force microscope (N9498S, Agilent Technologies, U.K.) operated in the contact mode under ambient conditions.

Water contact angle measurements were performed on the steel surfaces uncorroded and corroded in 15 wt % HCl solution without and with 1000 mg/L NDTHDC or 100 mg/L poly-NDTHDC at 90 °C for 6 h. The contact angles of a drop of water (3 μL) on the sample surfaces were measured by the sessile drop method with the Attension Contact Angle Meter (Biolin Scientific Instrument).

Ultraviolet−visible (UV−vis) experiments were also carried out to gain insights into the mechanism of interaction between the inhibitor molecules and the steel surface. In view of this, the absorbance characteristics of 15 wt % HCl solution + NDTHDC or poly-NDTHDC before and after API X60 steel sample immersion were collected utilizing a JASCO770-UV−vis spectrophotometer (200−650 nm) operated at a resolution of 1 nm with a scan rate of 200 nm/min.

The stability of the synthesized polymer was carried out using the thermogravimetric analysis (TGA) instrument, Discovery 972000.901 model, at a temperature range of 30−400 °C.

■ DATA AVAILABILITY

The raw/processed data required to reproduce these findings cannot be shared at this time as the data also forms part of an ongoing study.

■ ASSOCIATED CONTENT

Ⓢ Supporting Information

The Supporting Information is available free of charge at https://pubs.acs.org/doi/10.1021/acsomega.0c02345.

1H NMR spectra of NDTHDC and poly-NDTHDC (Figure S1); 13C NMR spectra of NDTHDC and poly-NDTHDC (Figure S2) (PDF)

■ AUTHOR INFORMATION

Corresponding Authors

Saviour A. Umoren − *Center of Research Excellence in Corrosion, Research Institute, King Fahd University of Petroleum and Minerals, Dhahran 31261, Saudi Arabia;* ⓞ orcid.org/0000-0002-8564-4897; Email: umoren@kfupm.edu.sa

Shaikh A. Ali − *Department of Chemistry, King Fahd University of Petroleum and Minerals, Dhahran 31261, Saudi Arabia;* ⓞ orcid.org/0000-0001-6628-7428; Email: shaikh@kfupm.edu.sa

Authors

Nurudeen A. Odewunmi − *Department of Chemistry, King Fahd University of Petroleum and Minerals, Dhahran 31261, Saudi Arabia*

Moses M. Solomon − *Center of Research Excellence in Corrosion, Research Institute, King Fahd University of Petroleum and Minerals, Dhahran 31261, Saudi Arabia;* ⓞ orcid.org/0000-0002-3251-8846

Complete contact information is available at:
https://pubs.acs.org/10.1021/acsomega.0c02345

Notes

The authors declare no competing financial interest.

■ REFERENCES

(1) Asiri, K. S.; Atwi, M. A.; Bueno, O. J.; Lecerf, B.; Pena, A.; Lesko, T.; Mueller, F.; Alexander, Z. I.; Pereira, F. T. C. Stimulating Naturally Fractured Carbonate Reservoirs. *Oilfield Rev.* **2013**, *25*, 1−17.

(2) Yang, Z.; Wang, Y.; Zhan, F.; Wang, R.; Chen, W.; Ding, M.; Hou, B. Investigation of High-Efficient Acidizing Inhibitors: Structure and Anti-Corrosion Performance of Novel Indolizine Derivatives. In *CORROSION*; NACE International, 2019.

(3) Singh, A.; Quraishi, M. A. Acidizing Corrosion Inhibitors: A Review. *J. Mater. Environ. Sci.* **2015**, *6*, 224−235.

(4) Frenler, F. B.; Growcock, W. W.; Lopp, V. R. *Mechanisms of Corrosion Inhibitors Used in Acidizing Wells*; SPE Production Engineering, 1988; pp 584−590.

(5) Ali, S. A.; El-Sharif, A. M. Z. Novel Class of Bisquaternary Ammonium Salts in Inhibition of Mild Steel Corrosion in HCl and H2SO4. *Corros. Eng., Sci. Technol.* **2012**, *47*, 265−271.

(6) Zhang, J.; Sun, X.; Ren, Y.; Du, M. The Synergistic Effect between Imidazoline-Based Dissymmetric Bis-Quaternary Ammonium Salts and Thiourea against CO2 Corrosion at High Temperature. *J. Surfactants Deterg.* **2015**, *18*, 981−987.

(7) Finšgar, M.; Jackson, J. Application of Corrosion Inhibitors for Steels in Acidic Media for the Oil and Gas Industry: A Review. *Corros. Sci.* **2014**, *86*, 17−41.

(8) Nations, U. *Globally Harmonized System of Classification and Labelling of Chemicals (GHS)*, 6th ed.; 2015.

(9) Alhaffar, M. T.; Umoren, S. A.; Obot, I. B.; Ali, S. A.; Solomon, M. M. Studies of the Anticorrosion Property of a Newly Synthesized Green Isoxazolidine for API 5L X60 Steel in Acid Environment. *J. Mater. Res. Technol.* **2019**, *8*, 4399−4416.

(10) Yang, Z.; Wang, Y.; Wang, R.; Chen, W.; Ding, M. *Insight of New Eco-Friendly Acidizing Corrosion Inhibitor: Structure and Inhibition of the Indolizine Derivatives*, Paper No.: SPE-193555-MS; Society of Petroleum Engineers, 2019; pp 1−11.

(11) Singh, A. *Pyran Derivatives as Acidizing Corrosion Inhibitors for N80 Steel in Hydrochloric Acid: Theoretical and Experimental Approaches*, Paper No. 12835; NACE International, 2019.

(12) Umoren, S. A.; Solomon, M. M. Polymeric Corrosion Inhibitors for Oil and Gas Industry. In *Corrosion Inhibitors in the Oil and Gas Industry*, Saji, V. S.; Umoren, S. A., Eds.; Wiley, 2020; Vol. *1*, pp 303−320.

(13) Umoren, S. A.; Solomon, M. M.; Ali, S. A.; Dafalla, H. D. M. Synthesis, Characterization, and Utilization of a Diallylmethylamine-Based Cyclopolymer for Corrosion Mitigation in Simulated Acidizing Environment. *Mater. Sci. Eng., C* **2019**, *100*, 897−914.

(14) Tian, Q.; Liu, Z.; Zhu, Y.; Dong, X.; Saih, Y.; Basset, J. M.; Sun, M.; Xu, W.; Zhu, L.; Zhang, D.; Huang, J.; Meng, X.; Xiao, F. S.; Han, Y. Beyond Creation of Mesoporosity: The Advantages of Polymer-Based Dual-Function Templates for Fabricating Hierarchical Zeolites. *Adv. Funct. Mater.* **2016**, *26*, 1881−1891.

(15) Butler, G. B. Cyclopolymerization. *J. Polym. Sci., Part A: Polym. Chem.* **2000**, *38*, 3451−3461.

(16) Kudaibergenov, S.; Jaeger, W.; Laschewsky, A. Polymeric Betaines: Synthesis, Characterization, and Application. *Adv. Polym. Sci.* **2006**, *201*, 157−224.

(17) Singh, P. K.; Singh, V. K.; Singh, M. Zwitterionic Polyelectrolytes: A Review. *e-Polym.* **2007**, *7*, 1−34.

(18) Ali, S. A.; Al-Hamouz, O. C. S. Comparative Solution Properties of Cyclocopolymers Having Cationic, Anionic, Zwitterionic and Zwitterionic/Anionic Backbones of Similar Degree of Polymerization. *Polymer* **2012**, *53*, 3368−3377.

(19) Yaocheng, Y.; Caihong, Y.; Singh, A.; Lin, Y. Electrochemical Study of Commercial and Synthesized Green Corrosion Inhibitors for N80 Steel in Acidic Liquid. *New J. Chem.* **2019**, *43*, 16058−16070.

(20) Farag, A. A.; Hegazy, M. A. Synergistic Inhibition Effect of Potassium Iodide and Novel Schiff Bases on X65 Steel Corrosion in 0.5M H2SO4. *Corros. Sci.* **2013**, *74*, 168−177.

(21) Abd El-Lateef, H. M. Corrosion Inhibition Characteristics of a Novel Salycilidene Isatin Hydrazine Sodium Sulfonate on Carbon Steel in HCl and a Synergistic Nickel Ions Additive: A Combined Experimental and Theoretical Perspective. *Appl. Surf. Sci.* **2020**, *501*, No. 144237.

(22) Solomon, M. M.; Umoren, S. A.; Quraishi, M. A.; Tripathi, D.; Abai, E. J. Effect of Akyl Chain Length, Flow, and Temperature on the Corrosion Inhibition of Carbon Steel in a Simulated Acidizing Environment by an Imidazoline-Based Inhibitor. *J. Pet. Sci. Eng.* **2020**, *187*, No. 106801.

(23) Oguzie, E. E. Corrosion Inhibition of Aluminium in Acidic and Alkaline Media by Sansevieria Trifasciata Extract. *Corros. Sci.* **2007**, *49*, 1527−1539.

(24) Oguzie, E. E.; Li, Y.; Wang, F. H. Corrosion Inhibition and Adsorption Behavior of Methionine on Mild Steel in Sulfuric Acid and Synergistic Effect of Iodide Ion. *J. Colloid Interface Sci.* **2007**, *310*, 90−98.

(25) Han, T.; Guo, J.; Zhao, Q.; Wu, Y.; Zhang, Y. Enhanced Corrosion Inhibition of Carbon Steel by Pyridyl Gemini Surfactants with Different Alkyl Chains. *Mater. Chem. Phys.* **2020**, *240*, No. 122156.

(26) Cao, S.; Liu, D.; Ding, H.; Wang, J.; Lu, H.; Gui, J. Task-Specific Ionic Liquids as Corrosion Inhibitors on Carbon Steel in 0.5 M HCl Solution: An Experimental and Theoretical Study. *Corros. Sci.* **2019**, *153*, 301−313.

(27) Corrales-Luna, M.; Le Manh, T.; Romero-Romo, M.; Palomar-Pardavé, M.; Arce-Estrada, E. M. 1-Ethyl 3-Methylimidazolium Thiocyanate Ionic Liquid as Corrosion Inhibitor of API 5L X52 Steel in H 2 SO 4 and HCl Media. *Corros. Sci.* **2019**, *153*, 85−99.

(28) Shao, S.; Wu, B.; Wang, P.; He, P.; Qu, X. P. Investigation on Inhibition of Ruthenium Corrosion by Glycine in Alkaline Sodium Hypochlorite Based Solution. *Appl. Surf. Sci.* **2020**, *506*, No. 144976.

(29) Song, J.; Bazant, M. Z. Effects of Nanoparticle Geometry and Size Distribution on Diffusion Impedance of Battery Electrodes. *J. Electrochem. Soc.* **2013**, *160*, A15.

(30) Brug, G. J.; van den Eeden, A. L. G.; Sluyters-Rehbach, M.; Sluyters, J. H. The Analysis of Electrode Impedances Complicated by the Presence of a Constant Phase Element. *J. Electroanal. Chem. Interfacial Electrochem.* **1984**, *176*, 275−295.

(31) Hashim, N. Z. N.; Anouar, E. H.; Kassim, K.; Zaki, H. M.; Alharthi, A. I.; Embong, Z. XPS and DFT Investigations of Corrosion Inhibition of Substituted Benzylidene Schiff Bases on Mild Steel in Hydrochloric Acid. *Appl. Surf. Sci.* **2019**, *476*, 861−877.

(32) Obot, I. B.; Onyeachu, I. B.; Umoren, S. A.; Quraishi, M. A.; Sorour, A. A.; Chen, T.; Aljeaban, N.; Wang, Q. High Temperature Sweet Corrosion and Inhibition in the Oil and Gas Industry: Progress, Challenges and Future Perspectives. *J. Pet. Sci. Eng.* **2019**, *185*, No. 106469.

(33) Ituen, E. B.; Asuquo, J. E. Inhibition of X80 Steel Corrosion in Oilfield Acidizing Environment Using 3-(2-Chloro-5,6-Dihydrobenzo[b][1]Benzazepin-11-Yl)-N,N-Dimethylpropan-1-Amine and Its Blends. *J. King Saud Univ., Sci.* **2019**, *31*, 127−135.

(34) Ituen, E.; Akaranta, O.; James, A. Corrosion Inhibition Characteristics of 2-[(E)-[5-Methoxy-1-[4-(Trifluoromethyl)Phenyl]-Pentylidene]Amino]Oxyethanamine on Steel in Simulated Oilfield Acidizing Solution. *J. King Saud Univ., Eng. Sci.* **2019**, *31*, 191−199.

(35) Onyeachu, I. B.; Solomon, M. M.; Umoren, S. A.; Obot, I. B.; Sorour, A. A. Corrosion Inhibition Effect of a Benzimidazole Derivative on Heat Exchanger Tubing Materials during Acid Cleaning of Multistage Flash Desalination Plants. *Desalination* **2019**, *479*, No. 114283.

(36) Solomon, M. M.; Umoren, S. A.; Quraishi, M. A.; Jafar Mazumder, M. A. Corrosion Inhibition of N80 Steel in Simulated

Acidizing Environment by N-(2-(2-Pentadecyl-4,5-Dihydro-1H-Imidazol-1-YL) Ethyl) Palmitamide. *J. Mol. Liq.* **2019**, *273*, 476−487.

(37) Solomon, M. M.; Umoren, S. A.; Quraishi, M. A.; Salman, M. Myristic Acid Based Imidazoline Derivative as Effective Corrosion Inhibitor for Steel in 15% HCl Medium. *J. Colloid Interface Sci.* **2019**, *551*, 47−60.

(38) Obot, I. B.; Onyeachu, I. B.; Umoren, S. A. Alternative Corrosion Inhibitor Formulation for Carbon Steel in CO2-Saturated Brine Solution under High Turbulent Flow Condition for Use in Oil and Gas Transportation Pipelines. *Corros. Sci.* **2019**, *159*, No. 108140.

(39) Onyeachu, I. B.; Obot, I. B.; Sorour, A. A.; Abdul-Rashid, M. I. Green Corrosion Inhibitor for Oilfield Application I: Electrochemical Assessment of 2-(2-Pyridyl) Benzimidazole for API X60 Steel under Sweet Environment in NACE Brine ID196. *Corros. Sci.* **2019**, *150*, 183−193.

(40) Douadi, T.; Hamani, H.; Daoud, D.; Al-Noaimi, M.; Chafaa, S. Effect of Temperature and Hydrodynamic Conditions on Corrosion Inhibition of an Azomethine Compounds for Mild Steel in 1 M HCl Solution. *J. Taiwan Inst. Chem. Eng.* **2017**, *71*, 388−404.

(41) Kosari, A.; Moayed, M. H.; Davoodi, A.; Parvizi, R.; Momeni, M.; Eshghi, H.; Moradi, H. Electrochemical and Quantum Chemical Assessment of Two Organic Compounds from Pyridine Derivatives as Corrosion Inhibitors for Mild Steel in HCl Solution under Stagnant Condition and Hydrodynamic Flow. *Corros. Sci.* **2014**, *78*, 138−150.

(42) Solmaz, R.; Kardaş, G.; Çulha, M.; Yazici, B.; Erbil, M. Investigation of Adsorption and Inhibitive Effect of 2-Mercaptothiazoline on Corrosion of Mild Steel in Hydrochloric Acid Media. *Electrochim. Acta* **2008**, *53*, 5941−5952.

(43) Jing, C.; Wang, Z.; Gong, Y.; Huang, H.; Ma, Y.; Xie, H.; Li, H.; Zhang, S.; Gao, F. Photo and Thermally Stable Branched Corrosion Inhibitors Containing Two Benzotriazole Groups for Copper in 3.5 wt % Sodium Chloride Solution. *Corros. Sci.* **2018**, *138*, 353−371.

(44) Zhang, Q. H.; Hou, B. S.; Li, Y. Y.; Zhu, G. Y.; Liu, H. F.; Zhang, G. A. Two Novel Chitosan Derivatives as High Efficient Eco-Friendly Inhibitors for the Corrosion of Mild Steel in Acidic Solution. *Corros. Sci.* **2019**, *164*, No. 108346.

(45) Samide, A.; Negrila, C.; Trandafir, I.; Maxut, A. Effect of Sulfacetamide on the Composition of Corrosion Products Formed onto Carbon Steel Surface in Hydrochloric Acid. *Dig. J. Nanomater. Biostructures* **2011**, *6*, 663−673.

(46) Samide, A.; Tutunaru, B.; Dobritescu, A.; Negrila, C. Study of the Corrosion Products Formed on Carbon Steel Surface in Hydrochloric Acid Solution. *J. Therm. Anal. Calorim.* **2012**, *110*, 145−152.

(47) He, X.; Jiang, Y.; Li, C.; Wang, W.; Hou, B.; Wu, L. Inhibition Properties and Adsorption Behavior of Imidazole and 2-Phenyl-2-Imidazoline on AA5052 in 1.0M HCl Solution. *Corros. Sci.* **2014**, *83*, 124−136.

(48) Wen, T. M.; Hou, K. H.; Bai, C. Y.; Ger, M. D.; Chien, P. H.; Lee, S. J. Corrosion Behaviour and Characteristics of Reforming Chromized Coatings on SS 420 Steel in the Simulated Environment of Proton Exchange Membrane Fuel Cells. *Corros. Sci.* **2010**, *52*, 3599−3608.

(49) De Souza, F. S.; Giacomelli, C.; Gonçalves, R. S.; Spinelli, A. Adsorption Behavior of Caffeine as a Green Corrosion Inhibitor for Copper. *Mater. Sci. Eng., C* **2012**, *32*, 2436−2444.

(50) Solomon, M. M.; Umoren, S. A.; Abai, E. J. Poly(Methacrylic Acid)/Silver Nanoparticles Composites: In-Situ Preparation, Characterization and Anticorrosion Property for Mild Steel in H_2SO_4 Solution. *J. Mol. Liq.* **2015**, *212*, 340−351.

(51) Umoren, S. A.; Solomon, M. M. Protective Polymeric Films for Industrial Substrates: A Critical Review on Past and Recent Applications with Conducting Polymers and Polymer Composites/Nanocomposites. *Prog. Mater. Sci.* **2019**, *104*, 380−450.

(52) Lgaz, H.; Chung, I. M.; Salghi, R.; Ali, I. H.; Chaouiki, A.; El Aoufir, Y.; Khan, M. I. On the Understanding of the Adsorption of Fenugreek Gum on Mild Steel in an Acidic Medium: Insights from Experimental and Computational Studies. *Appl. Surf. Sci.* **2019**, *463*, 647−658.

(53) Ahanotu, C. C.; Onyeachu, I. B.; Solomon, M. M.; Chikwe, I. S.; Chikwe, O. B.; Eziukwu, C. A. Pterocarpus Santalinoides Leaves Extract as a Sustainable and Potent Inhibitor for Low Carbon Steel in a Simulated Pickling Medium. *Sustainable Chem. Pharm.* **2020**, *15*, No. 100196.

(54) ASTM International, *Standard Practice for Preparing, Cleaning, and Evaluating Corrosion Test*, 2011; pp 1−9.

(55) NACE International, *Laboratory Corrosion Testing of Metals in Static Chemical Cleaning Solutions at Temperatures below 93 °C (200 °F)*, TM0193-2016-SG, 2000.